Available online at www.sciencedirect.com

SciVerse ScienceDirect

Ceramics International 39 (2013) 7641–7648

CERAMICS INTERNATIONAL

www.elsevier.com/locate/ceramint

The fabrication and characterization of sintered diatomite for potential microfiltration applications

Jang-Hoon Ha*, Eunji Oh, In-Hyuck Song

Powder and Ceramics Division, Korea Institute of Materials Science, 797 Changwondaero, Seongsan-gu, Changwon, Gyeongnam 642-831, Republic of Korea

Received 7 February 2013; received in revised form 21 February 2013; accepted 22 February 2013
Available online 14 March 2013

Abstract

Porous ceramic membranes have lately become a subject of special interest due to their outstanding thermal and chemical stability. We investigated whether a sintered diatomite support layer could also serve as a separation layer to minimize any processing difficulties, and investigated whether the support layer and the separation layer could be made from the same material to avoid a thermal mismatch during a high-temperature sintering process. We prepared sintered diatomite as a porous ceramic membrane for microfiltration, as diatomite particles are inherently porous and irregular. The pore characteristics of the sintered diatomite specimens were studied by scanning electron micrography, mercury porosimetry, and capillary flow porosimetry.
© 2013 Elsevier Ltd and Techna Group S.r.l. All rights reserved.

Keywords: A. Sintering; B. Porosity; E. Membranes; Coating; Diatomite

1. Introduction

The importance of porous ceramics has recently been recognized as researchers seek to exploit their unique properties, such as their high melting point, high corrosion resistance, high wear resistance, low density, low thermal conductivity, and low dielectric constant. In particular, porous ceramic membranes are feasible materials for the creation of porous ceramics. The driving force behind the development of porous ceramic membranes is mainly the need to produce membranes with greater levels of thermal and chemical stability, as most polymeric membranes cannot withstand operating temperatures above 200 °C or exposure to organic solvents such as benzene or toluene [1].

In general, the most important aspects of a porous ceramic membrane are its permeation and separation properties. Therefore, precise control of the average pore size, and the largest pore size, while retaining acceptable permeation capabilities is important. A challenging area in the application of ceramic membranes is how to control, tailor, and characterize the pore characteristics; emphasis has been placed on various approaches that afford control over the microstructural features of both the separation layer and support layer, which ultimately determine the permeation properties of porous ceramic membranes. Although processing routes to produce porous ceramics have been extensively documented in the literature [2], the relationship between the pore characteristics and the membrane properties of porous ceramic membranes has not yet been established.

Moreover, ceramic membranes are usually composites consisting of several layers of one or more different ceramics. A porous ceramic membrane is thus usually fabricated through multiple steps. A support layer is initially prepared to provide mechanical strength for the membrane, if needed, followed by the coating of one or more intermediate layers on the support layer, after which a final separation layer is deposited. Each step involves a high-temperature sintering process, making the ceramic membrane fabrication procedure expensive and challenging. If the support layer can also serve as a separation layer, or if the support layer and separation layer can at least be made from the same material to avoid a thermal mismatch

*Corresponding author. Tel.: +82 55 280 3350; fax: +82 55 280 3392.
E-mail addresses: hjhoon@kims.re.kr, hjhoon@gmail.com (J.-H. Ha).

0272-8842/$ - see front matter © 2013 Elsevier Ltd and Techna Group S.r.l. All rights reserved.
http://dx.doi.org/10.1016/j.ceramint.2013.02.102

during the sintering process, processing becomes easier and the time and cost issues associated with processing are mitigated.

The applications and separation mechanisms of porous ceramic membranes correspond to the pore size of the membranes. As it is difficult to create a support layer with microporous or dense materials due to their low permeation characteristics, it is worthwhile to investigate porous ceramic membranes that consist of a support layer only or a support layer and a separation layer composed of the same macroporous material. Among the methods of reverse osmosis, nanofiltration, ultrafiltration, and microfiltration, we focused on microfiltration in this study, as the largest and smallest pore sizes of membranes for microfiltration are roughly several μm and 0.1 μm, respectively.

Recent developments in porous ceramic membranes have heightened the need to investigate mass transport through a separation layer deposited on a support layer, as the overall permeation capabilities and reliability of the pores on separation layer are critical to porous ceramic membrane applications. In general, the permeability of a separation layer on a support layer governs the overall permeation capabilities of the membrane. Although there have been various reports on commonly used materials for ceramic membranes, including Al_2O_3, TiO_2, ZrO_2, SiO_2, and composites of these materials, there have been few studies on 'porous and irregular' starting particles such as diatomite. Diatomite is a sedimentary rock originating from the siliceous fossilized skeletons of diatoms, which are composed of rigid cell walls called frustules. To date, no detailed studies on the use of a separation layer made with inherent porous and irregular particles have been published.

The present study investigated the following areas. First, we investigated whether a sintered diatomite support layer could simultaneously serve as a separation layer, within a sintering temperature range of 900–1200 °C. The basic properties of the sintered diatomite support layer and the processing conditions for additional experiments were obtained during these experiments. When a sintered porous ceramic is used as a surface membrane filter as a support layer, the largest pore size of the sintered layer is inconsequential. The important factors that must be considered for the sintered porous ceramic support layer are the mass transfer resistance, mechanical strength, and chemical resistance.

Second, to enhance the permeability of the sintered diatomite support layer further, spherical pores were incorporated using a sacrificial polymer template method. This type of method usually involves the preparation of a continuous matrix of ceramic particles and a dispersed sacrificial phase that is homogeneously distributed throughout the matrix and is ultimately extracted to generate pores within the microstructure. Hollow spheres were adopted as a sacrificial polymer template to minimize both the amount of the gas phase and the time to complete the pyrolysis process. However, because micro-cracks can be generated within the microstructure and act as escape paths for the gas phase generated during the pyrolysis of the polymer beads despite the adoption of hollow spheres instead of solid spheres to minimize micro-cracks, the largest pore size on the surface can fluctuate. Thus, we introduced a diatomite separation layer via a dip-coating process. We then investigated whether such a layer can suppress the fluctuation of the largest pore size of the diatomite support layer.

2. Material and methods

Diatomite (Celite 499, Celite Korea Co. Ltd., Korea) was used for the preparation of the sintered diatomite specimens. To reduce the average particle size of diatomite to less than 5 μm, distilled water was used as a solvent. The slurry was ball-milled for 24 h with a ball-to-powder volume ratio of 2:1. The diatomite particles maintained both the unique shapes and inherent pores of the fossilized skeleton of diatoms after being ball-milled for 24 h. For the support layer, green bodies of diatomite particles with a polyethylene glycol binder were dry-pressed at 18.7 MPa, after which sintering was carried out at 900–1200 °C for 1 h.

To enhance the permeability of the sintered diatomite support layer, spherical pores were incorporated into the layer by a sacrificial polymer template method. Diatomite particles ranging in quantity from 0 vol% to 25 vol% of Expancel (Hollow sphere, Expancel-092-DET-80-d25, Eka Chemicals AB, Sweden) as a sacrificial polymer template, distilled water, and a polyethylene glycol binder were mixed, wet-pressed at 18.7 MPa, and dried for 24 h. Next, they were sintered at 1200 °C for 1 h. To suppress the fluctuation of the largest pore size of the sintered diatomite support layer, a dip-coating process was carried out. For the separation layer, diatomite particles ball-milled for 24 h, distilled water, organic binder (HS BD-25, San Nopco Korea, Korea), and inorganic binder (AS-40, Sigma-Aldrich, USA) were mixed, dip-coated on a sintered diatomite support layer, dried at room temperature for 24 h, and then sintered at 1200 °C for 1 h.

The flexural strengths of the sintered diatomite specimens were measured by a three-point bending test (Instron 4206, Instron, USA). The pore characteristics were investigated by scanning electron micrography (JSM-5800, JEOL, Japan), mercury porosimetry (Autopore IV 9510, Micromeritics, USA) and capillary flow porosimetry (CFP-1200-AEL, Porous Materials Inc., USA).

3. Results and discussion

Typical scanning electron microscope (SEM) images of the diatomite support layers sintered at 1000 °C and 1200 °C for 1 h are shown in Fig. 1(a) and (b), respectively. These sintered diatomite specimens showed similar microstructures and maintained the unique shapes of the fossilized skeleton of the diatoms when sintered at temperatures up to 1200 °C. As shown in Fig. 2(a), the average pore size of the sintered diatomite increased slightly as the sintering temperature was increased from 900 °C to 1200 °C. Unlike the isolated pores in dense ceramics, in porous ceramics both the grains and the pores normally increase in size while decreasing in number. Generally, coarsening is used to describe the progress by

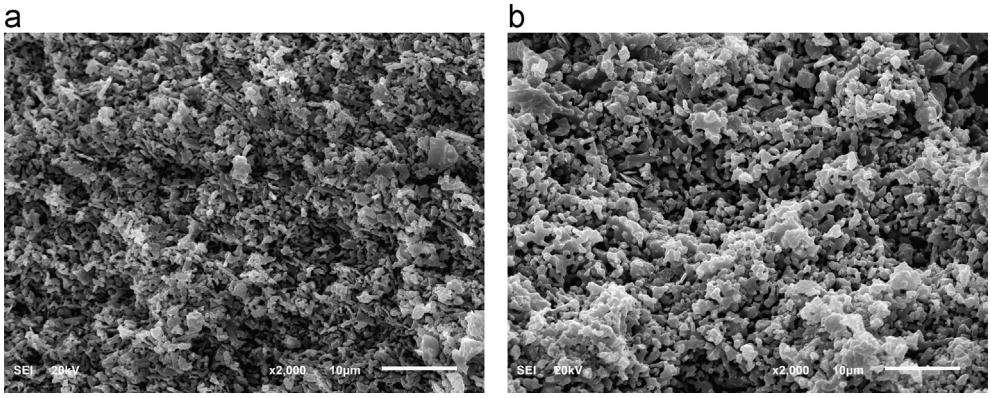

Fig. 1. Typical SEM images of diatomite support layers sintered for 1 h at (a) 1000 °C and (b) 1200 °C.

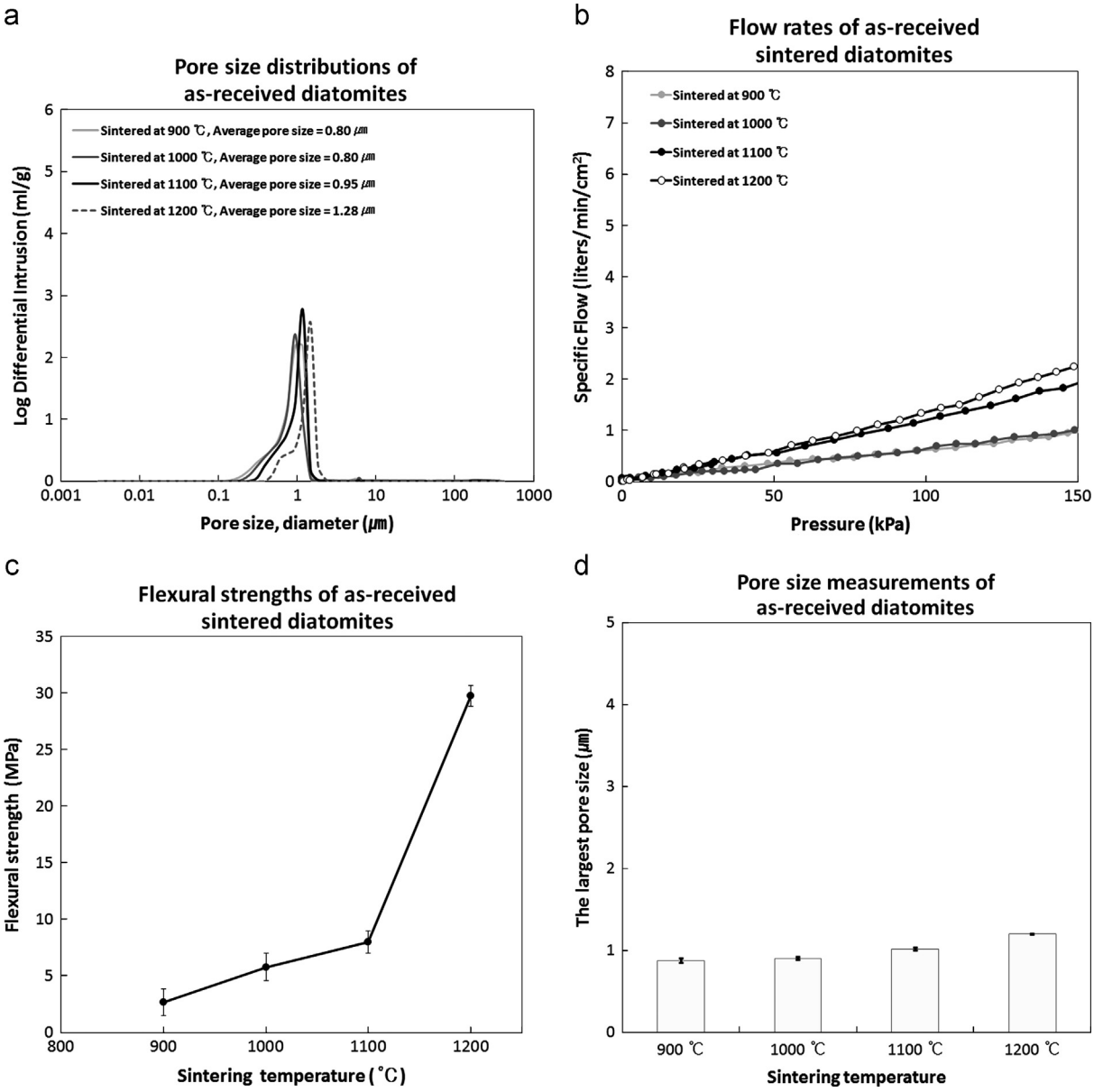

Fig. 2. (a) Pore size distributions, (b) air permeation properties, (c) flexural strengths, and (d) the largest pore size of the diatomite support layers sintered at temperatures ranging from 900 °C to 1200 °C.

which grains and pores grow. These trends are in good agreement with experimental results covering different porous ceramics, such as diatomite [3], silicon carbide [4,5], alumina [6], corundum–mullite [7] and zirconia [8] in different temperature ranges. Fig. 2(b) presents the air permeation properties of sintered diatomite support layers prepared at different sintering temperatures ranging from 900 °C to 1200 °C. The air permeation properties of the sintered diatomite support layers were proportional to the increase in the average pore size with sintering temperatures up to 1200 °C. We measured the air permeability of sintered diatomite support layers, however, at low flow rates; the air permeability of the specimens may be higher than the liquid permeation properties of the same specimens, as gas does not adhere to the pore walls as liquid does and because the slippage of gases along the pore walls gives rise to an apparent dependence of the permeation properties on the pressure in what is known as the Klinkenberg effect [9]. Therefore, to compare our results with the liquid permeation properties of typical ceramic microfiltration membranes reported in the literature, the pure water flux of the diatomite support layer sintered at 1200 °C was measured by capillary flow porosimetry. The pure water flux of the diatomite support layer sintered at 1200 °C was 6.3×10^4 L m^{-2} h^{-1} bar^{-1}. In the literature, the pure water flux of typical ceramic microfiltration membranes based on spherical fly ash [10], γ-alumina [11], and zirconia [12] were 1.6×10^4 L m^{-2} h^{-1} bar^{-1}, $\sim 1.0 \times 10^3$ L m^{-2} h^{-1} bar^{-1}, and 1.6×10^3 L m^{-2} h^{-1} bar^{-1}, respectively. As will be discussed below, the sintered diatomite support layer with no sacrificial polymer template had the lowest air permeation property. By the addition of the sacrificial polymer template, both the air permeation property and the pure water flux could be further enhanced. Thus, the permeability of the diatomite membrane exhibited in this study may be good enough for cross-flow microfiltration. In addition, while we focused on the air permeation properties of sintered diatomite supports, the liquid permeation properties of these supports represent an important issue for future research.

When the sintering temperature is less than 1100 °C, the flexural strength is proportional to the sintering temperature, as shown in Fig. 2(c). When the sintering temperature is greater than 1100 °C, the flexural strength increases sharply as the sintering temperature is increased further. This suggests that the preparation of sintered diatomite with a high mechanical strength is possible at a sintering temperature of 1200 °C or higher, as a slight increase in the sintering temperature dramatically increases the mechanical strength. The flexural strength of a typical ceramic microfiltration membrane based on alumina [13] or silicon carbide [4] is often above 50 MPa, and the flexural strengths of clay materials such as mullite [14], kaolin [15], and diatomite [16] are usually below 30 MPa. However, considering the high permeation properties, the low sintering temperature, and the low cost of the raw material, unlike those of high-purity alumina or silicon carbide, the flexural strength of a sintered diatomite support layer is likely to be feasible for microfiltration applications. In preliminary

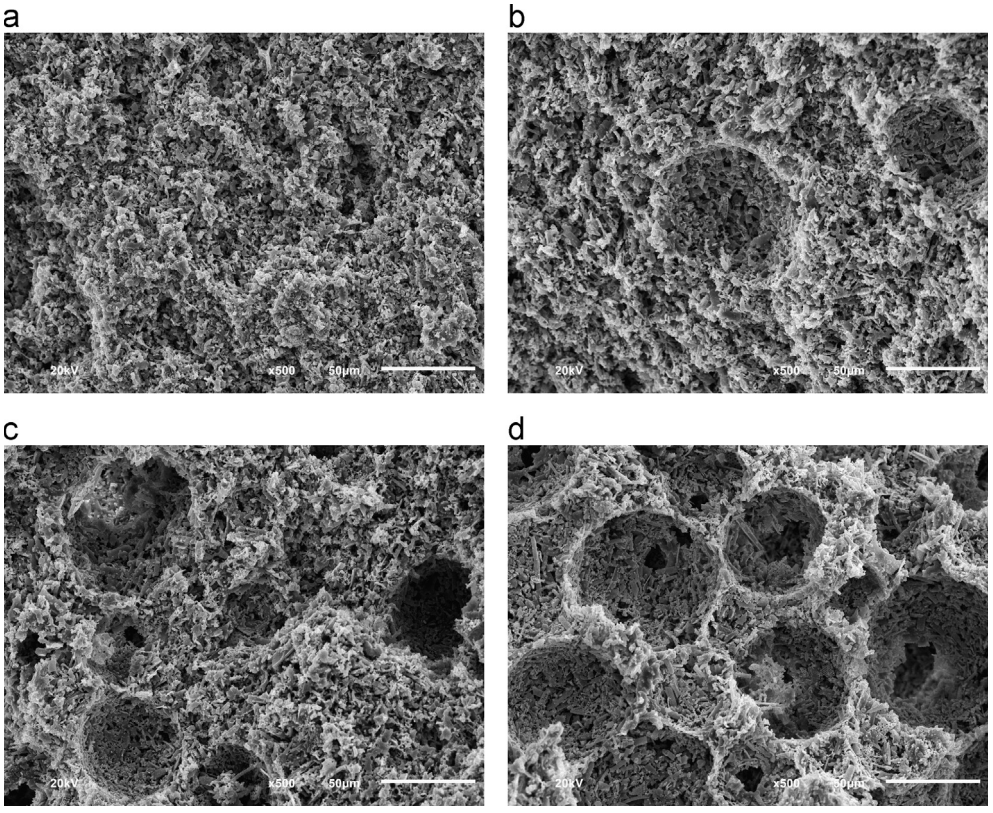

Fig. 3. Typical SEM images of the diatomite support layers sintered for 1 h at 1200 °C with (a) no addition of a sacrificial polymer template; (b) a 5 vol% sacrificial polymer template, (c) a 15 vol% sacrificial polymer template, and (d) a 25 vol% sacrificial polymer template.

experiments, the sintering of diatomite at a temperature of 1300 °C led to an increase in the mechanical strength; however, the air permeation property decreased considerably. Therefore, there is a trade-off between the mechanical strength and the permeation capabilities. Hence, taking into consideration the findings of the preliminary experiments and those in the literature [3], we found that sintered diatomite had similar microstructures up to 1200 °C. However, a clear coalescence of porous diatom frustules and grains in the specimens occurred at 1300 °C, and the average pore size consequently decreased. This suggests that the collapse of the inherent pore structure of diatomite at 1300 °C was induced by impurities in diatomite such as Na_2O, K_2O, Al_2O_3, CaO and MgO. These impurities favor low-temperature eutectics and thus the formation of a melt phase in the silica-rich grains [17]. Therefore, we could not expect a further enhancement of the air permeation properties of sintered diatomite by an increase in the average pore size when the sintering temperature exceeded 1200 °C. In this study, we limited the sintering temperature of diatomite to 1200 °C, as we wanted to focus on the enhancement of the air permeation properties of a sintered diatomite support which retains the unique shapes of the fossilized skeleton of diatoms and which make diatomite different from typical silica particles with impurities.

Fig. 2(d) shows the variation of the largest pore size of the diatomite sintered at temperatures ranging from 900 °C to

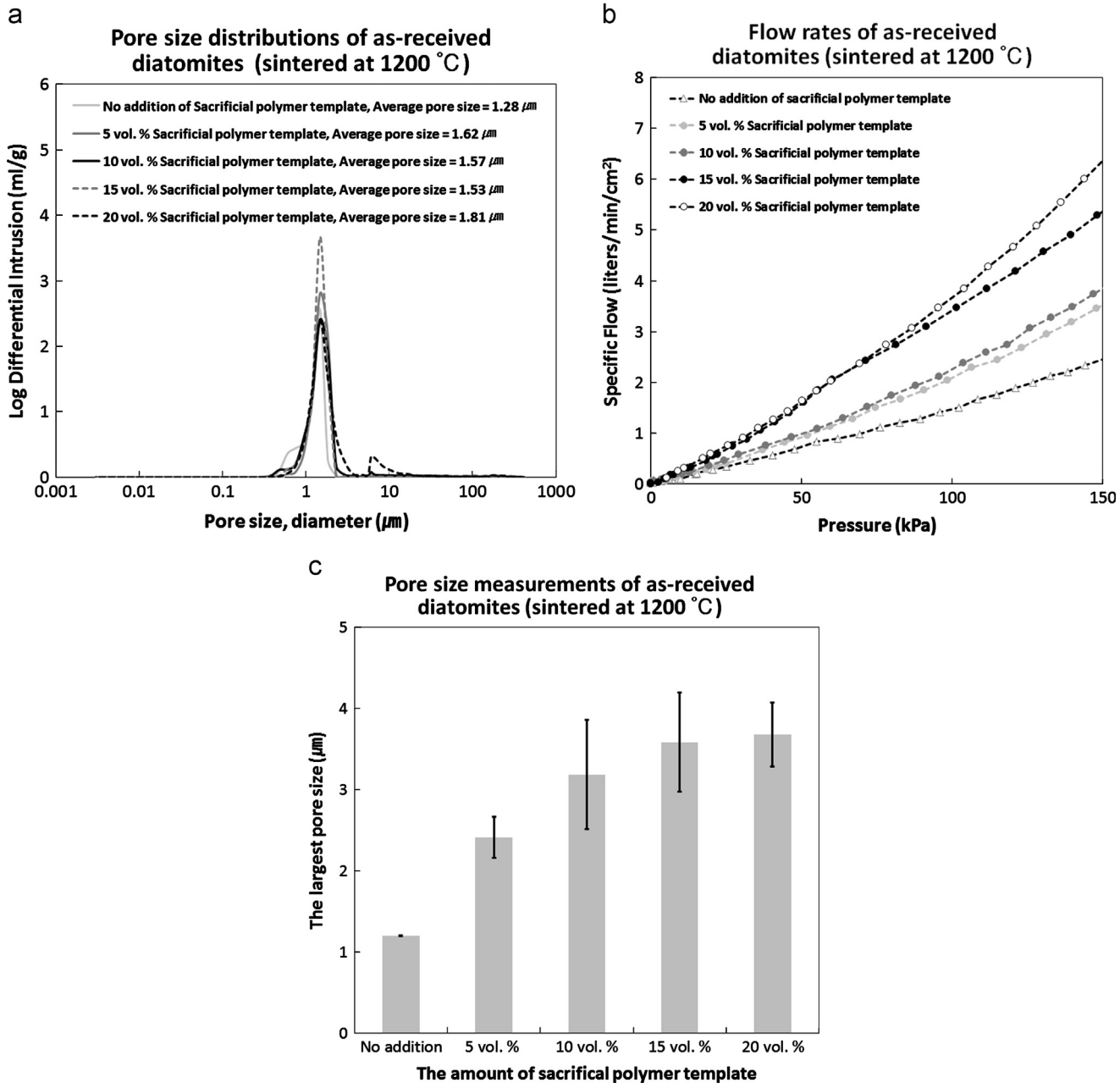

Fig. 4. (a) Pore size distributions, (b) air permeation properties, and (c) the largest pore size of diatomite support layers with varying amounts of sacrificial polymer template sintered for 1 h at 1200 °C.

1200 °C as measured by the bubble point method. The bubble point method is the most widely used approach for evaluating pore sizes. It is capable of determining the largest pore size of a membrane. It works based on the concept, for a given fluid and pore size under constant wetting, that the pressure required to force an air bubble through the pore is inversely proportional to the size of the pore. The largest pore size of the sintered diatomite remained at approximately 1 μm with negligible standard error regardless of the sintering temperature. Taking into account all of the experimental results above, that is, the air permeation properties, pore characteristics, and flexural strengths, the optimum sintering temperature is most likely 1200 °C.

Typical SEM images of the diatomite support layers in accordance with the amount of sacrificial polymer template, sintered for 1 h at 1200 °C, are shown in Fig. 3. Fig. 3(a) shows a support layer without a sacrificial polymer template; (b) shows a layer with a sacrificial polymer template at 5 vol%; (c) shows a layer with a sacrificial polymer template at 15 vol%, and (d) shows a layer with a sacrificial polymer template at 25 vol%. The microstructures of the sintered diatomite support layers prepared by the sacrificial polymer method show that the spherical pores are distributed in the diatomite matrix in a manner resembling Swiss cheese. For further experiments, the amount of sacrificial polymer template was confined to 20 vol%, because, in preliminary work, we also found that there is a trade-off between the mechanical strength and the permeation properties with an increase in the amount of sacrificial polymer template and with an increase in the sintering temperature.

Fig. 4(a) shows the pore size distributions of the sintered diatomite support layers prepared by the sacrificial polymer template method at a sintering temperature of 1200 °C according to the amount of sacrificial polymer template. When the sacrificial polymer template was added at amounts ranging from 5 to 15 vol%, similar average pore sizes were obtained, with one peak at around 1–5 μm. However, when the diatomite was sintered with 20 vol% of sacrificial polymer template, a peak at around 1–5 μm and another peak at around 10–20 μm appeared. The former corresponds to inter-particle voids between the diatomite particles, whereas the latter corresponds to the throats [18] or entrance openings of spherical pores, as mercury enters the spherical pores at a pressure determined by the entrance size rather than the actual spherical pore size. Fig. 4(b) presents the air permeation properties of sintered diatomite support layers prepared with various amounts of sacrificial polymer template. The air permeation properties of the sintered diatomite support layers were proportional to the amount of the sacrificial polymer template regardless of the average pore size and were enhanced relative to those of the sintered diatomite support layers prepared while controlling only the sintering temperature, as the average pore sizes measured by mercury porosimetry do not reflect the macroporous spherical pores induced by the sacrificial polymer template. However, the largest pore sizes of the sintered diatomite support layers were proportional to the increase in the amount of the sacrificial polymer template, as shown in Fig. 4(c). This is attributable to micro-cracks generated within the microstructure during the pyrolysis of the sacrificial polymer template or incomplete sintering induced by insufficient compaction due to the incursion of the sacrificial polymer template into the diatomite particles. Although we utilized hollow spheres instead of solid spheres to minimize the aforementioned effects, the largest pore sizes on the surface fluctuated with an excessive degree of standard error. For porous ceramic membrane applications, this degree of fluctuation of the largest pore size is undesirable. Therefore, as noted earlier, we applied a separation layer composed of the same diatomite by a dip-coating process.

Cross-section SEM images of the interface between the sintered diatomite support layer and the sintered diatomite separation layer are provided in Fig. 5(a) and (b). In the dip-coating process, the driving force for the coating is the capillary force of the porous substrate [19]. Therefore, the coating and bonding between the foam and substrate depended on the substrate morphology. When the support layer was porous, as shown in Fig. 5(a), the separation layer was expected to come into contact with the support layer due to capillary force. We also attempted the same coating procedures on a dense support layer. When the separation layer came into contact with the top surface of the dense support layer, the coated separation layer was easily detached, as there were no pores to provide capillary force. Fig. 5(b) shows that the lower

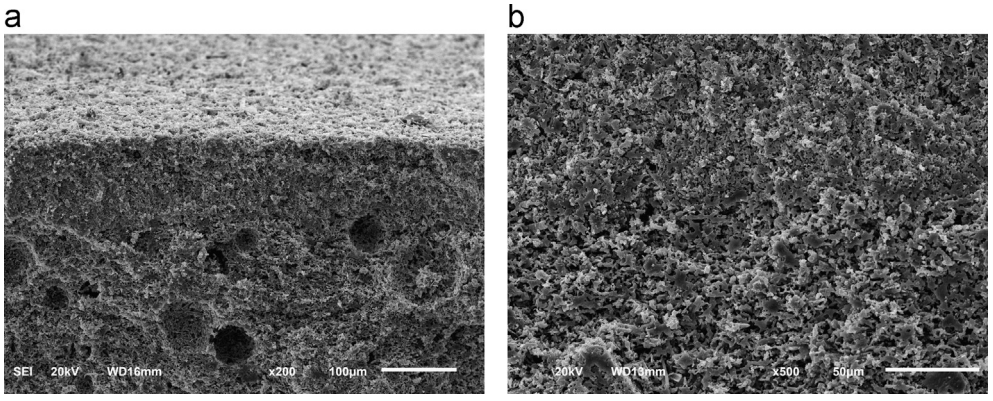

Fig. 5. Typical SEM images of (a) the cross-section of the interface between a separation layer and a support layer sintered for 1 h at 1200 °C, and (b) high magnification of (a).

half of the image (the sintered diatomite support layer) has larger grains than the upper half (the dip-coated and then sintered diatomite separation layer). Although both the support layer and the separation layer were prepared from the same diatomite material, the support layer was exposed to a high temperature for larger duration, when the separation layer was sintered. Therefore, grain growth progressed more favorably in the support layer with an increased period of thermal exposure. Also, it is important to note that the bottom surface of the separation layer and the top surface of the support layer were joined microscopically.

Fig. 6(a) shows that the air permeation properties of the sintered diatomite supports with separation layers, prepared by varying the amount of sacrificial polymer template from no addition to 20 vol%, and then sintered at 1200 °C. Although there is a general decline in properties due to the presence of the separation layer, the air permeation properties of the sintered diatomite are proportional to the increased amount of sacrificial polymer template. Possibly due to inter-particle voids induced by the irregular shape of the diatomite particles, the permeation characteristics of the sintered diatomite separation layer were different from those of a conventional dense ceramic separation layer. Fig. 6(b) shows the largest pore sizes of sintered diatomite varying with the sintering temperature from 900 °C to 1200 °C, as measured by the bubble point method. The largest pore sizes of the sintered diatomite remained at around 1 μm with negligible standard error, regardless of the amount of sacrificial polymer template.

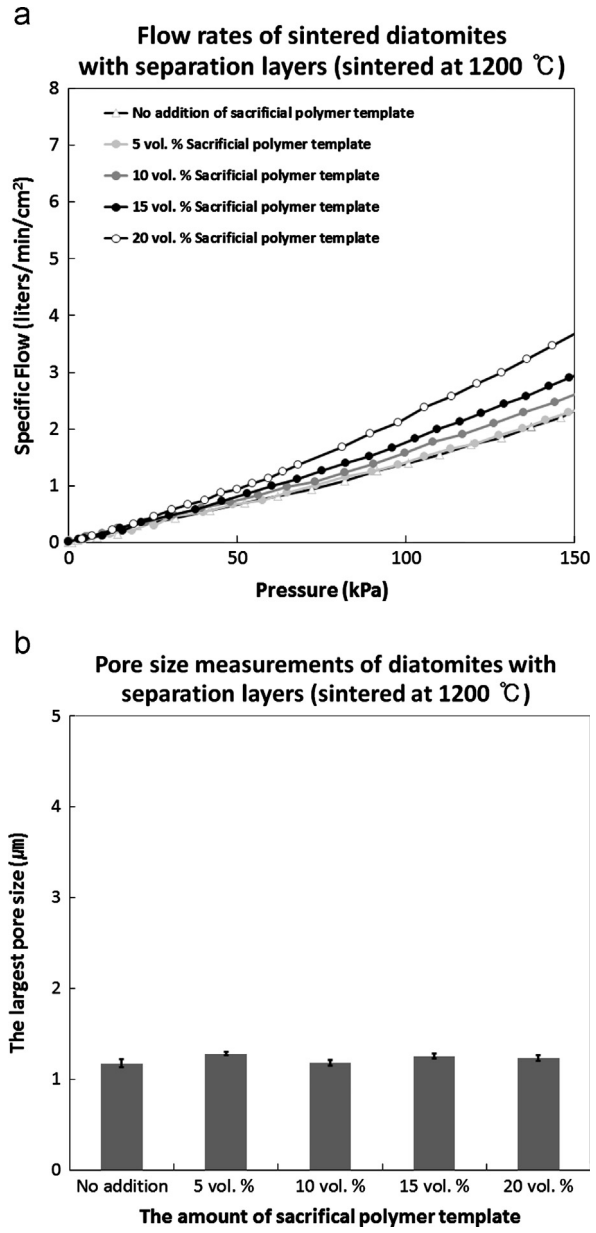

Fig. 6. (a) The air permeation properties, and (b) the largest pore size of the diatomite support layers with a diatomite separation layer while varying the amount of the sacrificial polymer template, and sintered for 1 h at 1200 °C.

4. Conclusion

In summary, the air permeation properties of sintered diatomite support layers were proportional to the increase in the average pore size at sintering temperatures up to 1200 °C. The largest pore sizes of sintered diatomite remained at around 1 μm with negligible standard error, regardless of the sintering temperature. The air permeation properties of the sintered diatomite support layers were proportional to the amount of the sacrificial polymer template regardless of the average pore size, and they increased relative to those of a sintered diatomite support layer prepared when controlling only the sintering temperature. However, the largest pore sizes of the sintered diatomite support layers were proportional to the increased amount of sacrificial polymer template, with excessive standard error. To suppress this fluctuation of the largest pore size, we adopted a separation layer composed of the same diatomite that was deposited by a dip-coating process. The largest pore sizes of the sintered diatomite remained at around 1 μm with negligible standard error regardless of the amount of sacrificial polymer template at the expense overall of a slight decrease of the air permeation properties.

It is noteworthy that the air permeation properties of sintered diatomite support layers could be enhanced by tailoring the pore structures. Furthermore, the largest pore sizes of the sintered diatomite support layers could be controlled by adopting a diatomite separation layer. These findings show the feasibility of using sintered diatomite as a porous ceramic membrane for microfiltration.

Acknowledgments

This study was supported financially by the Fundamental Research Program of the Korean Institute of Materials Science (KIMS).

References

[1] L. Kang, Ceramic Membranes for Separation and Reaction, John Wiley & Sons, Ltd., London, 2007.

[2] A.R. Studart, U.T. Gonzenbach, E. Tervoort, L.J. Gauckler, Processing routes to macroporous ceramics: a review, Journal of the American Ceramic Society 89 (2006) 1771–1789.
[3] N. van Garderen, F.J. Clemens, M. Mezzomo, C.P. Bergmann, T. Graule, Investigation of clay content and sintering temperature on attrition resistance of highly porous diatomite based material, Applied Clay Science 52 (2011) 115–121.
[4] P.K. Lin, D.S. Tsai, Preparation and analysis of a silicon carbide composite membrane, Journal of the American Ceramic Society 80 (1997) 365–372.
[5] J.H. Eom, Y.W. Kim, I.H. Song, H.D. Kim, Processing and properties of polysiloxane-derived porous silicon carbide ceramics using hollow microspheres as templates, Journal of the European Ceramic Society 28 (2008) 1029–1035.
[6] A. Pruchnewski, Effect of sintering temperature on functional properties of alumina membranes, Journal of the European Ceramic Society 22 (2002) 613–623.
[7] W. Yan, N. Li, B. Han, Effects of sintering temperature on pore characterization and strength of porous corundum–mullite ceramics, Journal of Ceramic Processing Research 11 (2010) 388–391.
[8] D. Sen, T. Mahata, A.K. Patra, S. Mazumder, B.P. Sharma, Effect of sintering temperature on pore growth in ZrO_2–8 mol% Y_2O_3 ceramic compact prepared by citric acid gel route: a small-angle neutron scattering investigation, Journal of Alloys and Compounds 364 (2004) 304–310.
[9] W. Tanikawa, T. Shimamoto, Comparison of Klinkenberg-corrected gas permeability and water permeability in sedimentary rocks, International Journal of Rock Mechanics and Mining Sciences 46 (2009) 229–238.
[10] J. Fang, G. Qin, W. Wei, X. Zhao, L. Jiang, Elaboration of new ceramic membrane from spherical fly ash for microfiltration of rigid particle suspension and oil-in-water emulsion, Desalination 311 (2013) 113–126.
[11] S.S. Madaeni, H. Ahmadi Monfared, V. Vatanpour, A. Arabi Shamsabadi, E. Salehi, P. Daraei, S. Laki, S.M. Khatami, Coke removal from petrochemical oily wastewater using γ-Al_2O_3 based ceramic microfiltration membrane, Desalination 293 (2012) 87–93.
[12] F. Bouzerara, A. Harabi, B. Ghouil, N. Medjemem, B. Boudaira, S. Condom, Elaboration and properties of zirconia microfiltration membranes, Procedia Engineering 33 (2012) 278–284.
[13] C.-H. Chen, K. Takita, S. Ishiguro, S. Honda, H. Awaji, Fabrication on porous alumina tube by centrifugal molding, Journal of the European Ceramic Society 25 (2005) 3257–3264.
[14] O. Bakhtiari, M. Samei, H. Taghikarimi, T. Mohammadi, Preparation and characterization of mullite tubular membranes, Desalination and Water Treatment 36 (2011) 210–218.
[15] S. Jana, M.K. Purkait, K. Mohanty, Preparation and characterizations of ceramic microfiltration membrane: effect of inorganic precursors on membrane morphology, Separation Science and Technology 46 (2011) 33–45.
[16] P.V. Vasconcelos, J.A. Labrincha, J.M.F. Ferreira, Permeability of diatomite layers processed by different colloidal techniques, Journal of the European Ceramic Society 20 (2000) 201–207.
[17] F. Akhtar, Y. Rehman, L. Bergström, A study of the sintering of diatomaceous earth to produce porous ceramic monoliths with bimodal porosity and high strength, Powder Technology 201 (2010) 253–257.
[18] H. Giesche, Mercury porosimetry: a general (practical) overview, Particle and Particle Systems Characterization 23 (2006) 9–19.
[19] H.-J. Son, R.-H. Song, T.-H. Lim, S.-B. Lee, S.-H. Kim, D.-R. Shin, Effect of fabrication parameters on coating properties of tubular solid oxide fuel cell electrolyte prepared by vacuum slurry coating, Journal of Power Sources 195 (2010) 1779–1785.